Frontiers of Information Technology & Electronic Engineering
www.jzus.zju.edu.cn; engineering.cae.cn; www.springerlink.com
ISSN 2095-9184 (print); ISSN 2095-9230 (online)
E-mail: jzus@zju.edu.cn

An error-based observer improved by the repetitive control strategy for electro-optical tracking systems#

Mai TANG[1,2,3,4], Wenqiang XIA[1,2,3,4], Jiuqiang DENG[1,2,3,4], Yao MAO‡[1,2,3,4]

[1]*National Key Laboratory of Optical Field Manipulation Science and Technology, Chinese Academy of Sciences, Chengdu 610209, China*

[2]*Key Laboratory of Optical Engineering, Chinese Academy of Sciences, Chengdu 610209, China*

[3]*Institute of Optics and Electronics, Chinese Academy of Sciences, Chengdu 610209, China*

[4]*University of Chinese Academy of Sciences, Beijing 101408, China*

E-mail: tangmai22@mails.ucas.ac.cn; xiawenqiang20@mails.ucas.ac.cn; jqdeng@ioe.ac.cn; maoyao@ioe.ac.cn

Received Nov. 22, 2023; Revision accepted Apr. 16, 2024; Crosschecked Mar. 5, 2025

Abstract: Electro-optical tracking systems have been widely used in the cutting-edge domains of free space environment detection and communication owing to their exceptional performance. However, external disturbances often significantly impact the working accuracy of these systems. As their scope of application continues to broaden, increasingly complex operating conditions introduce more intricate environments and disturbances. This paper introduces a composite control structure of an enhanced error-based observer, rooted in the repetitive control strategy, tailored for two types of complex disturbances: periodic harmonic disturbance and narrow-band peak periodic disturbance. This structure not only ensures the system's stability, but also suppresses periodic disturbances across multiple frequencies, effectively addressing the challenge that current disturbance suppression methods face in mitigating complex periodic disturbances. Moreover, necessary proofs are provided and an experimental platform is established for the electro-optical system, demonstrating the efficacy and reliability of the proposed control methods under various conditions.

Key words: Disturbance suppression; Error-based observer; Repetitive control; Electro-optical tracking system; Specific frequency point

https://doi.org/10.1631/FITEE.2300796 **CLC number:** TP273

1 Introduction

The electro-optical tracking system refers to a comprehensive optical instrument that integrates mechanical structures, electronic power, control system, and other structures. It has been widely used in biomedicine, aerospace, astronomical observations, quantum computing, microstructure characterization, long-distance information transmission, and other fields (Berkefeld et al., 2010; Beaulieu-Laroche et al., 2021; Madsen et al., 2022; Kalita et al., 2023; Snigirev et al., 2023). For the control of the electro-optical tracking system, the main purpose is to improve the stability (Downey and Stockum, 1989; Li et al., 2022) and to enhance the disturbance suppression ability while ensuring the stability of the system (Zhao et al., 2023). As the mobile platform gradually becomes the application carrier of the electro-optical system (Kennedy and Kennedy, 2003; Ricks et al., 2004), the working characteristics of these carriers will directly affect the working accuracy of the electro-optical tracking system. The vibration of the mechanical structure, the fluctuation of the mobile

‡ Corresponding author

Electronic supplementary materials: The online version of this article (https://doi.org/10.1631/FITEE.2300796) contains supplementary materials, which are available to authorized users

ORCID: Mai TANG, https://orcid.org/0009-0000-4414-2412; Yao MAO, https://orcid.org/0000-0003-1785-2018

platform, the atmospheric disturbance around the work site, and other external factors will act as interference factors in the working process and affect the performance of the electro-optical system (Somaschini et al., 2019). These perturbations have complex properties, including periodic and aperiodic disturbances. Specifically, periodic disturbances may seriously affect the working process of the electro-optical tracking system (Deng et al., 2023).

Numerous researchers globally have conducted studies to address this issue (Caruso, 2001; Lu et al., 2024). For example, the use of disturbance feedforward control has been demonstrated to improve the stability of the stable platform and significantly enhance both the stability and disturbance suppression performance of the tracking platform (Ren et al., 2018). To address the time delay in the open-loop system, an enhanced disturbance rejection technique was proposed by Shamsuzzoha and Lee (2009). Furthermore, an adaptive disturbance rejection method was applied to adjust hard disk drives in the dead zone (Lee JS et al., 2016). Active disturbance rejection control (ADRC), a method designed to improve both the transient and immunity performances of systems plagued with uncertainties (Dong et al., 2018), incorporates an algorithm proposed to enhance the response speed through a model-assisted active disturbance rejection controller (Sobhy and Lei, 2021). Additionally, sliding mode control can effectively solve the buffeting problem and ensure the stability of the system in the process of disturbance suppression. Adaptive second-order sliding mode control has also been used for enhanced disturbance rejection for grid-connected neutral point clamped (NPC) converters (Shen et al., 2022).

The disturbance observer (DOB) features a simple structure, which enhances the disturbance suppression capabilities of the system by observing the disturbance signal and providing feedback (Deng et al., 2022). It also maintains the stability, demonstrating excellent comprehensive performance (Ohishi et al., 1987). Building upon this, a DOB control algorithm aimed at high-precision positioning systems and uncertain systems was proposed (Lee HS and Tomizuka, 1996; Chen and Tomizuka, 2013). However, despite the initial DOB structure improves disturbance suppression performance, it compromises the stability of the system. To address this problem, Deng et al. (2021) proposed a modified DOB model by adjusting the observer structure and filter parameters, which further enhanced DOB's performance in both disturbance suppression and target tracking across multiple degrees of freedom.

Inoue et al. (1981) proposed an early structure akin to repetitive control for managing the computer control of the three main ring magnets of a proton synchrotron with a thyristor power supply. Subsequently, Hara et al. (1988) officially introduced this control structure, termed repetitive control, to fulfill the performance requirements of the control system at the repetition frequency. Following this, Fedele and Ferrise (2014) and Lan et al. (2020) introduced an enhanced scheme by combining repetitive control with a fractional-order controller and preview compensation, respectively. Furthermore, Chen and Tomizuka (2013) and Tang et al. (2019) developed a new repetitive control structure, incorporating a nominal model. As a control method, repetitive control is capable of achieving high performance with periodic signals through a relatively simple structure. This approach has also been used to enhance the disturbance suppression capability.

Recent years have seen significant research on the modified repetitive controller, which has been proposed to address both theoretical and practical challenges. Longman (2000) suggested that linear iterative learning and repetitive control may have the same design criteria. Zhou L et al. (2020) introduced a modified repetitive control system to enhance disturbance rejection performance. Using the principles of repetitive control to refine the extended state observer enables effective disturbance suppression (Nie et al., 2021). This approach is independent of an exact system model, thereby ensuring the system's overall robustness. Furthermore, the concept of repetitive control has been adapted for nonlinear systems. Wang et al. (2020) developed a repetitive controller based on a fuzzy observer, employing a T-S fuzzy model to characterize the nonlinear system and address the tracking issue of periodic signals. In the context of a discrete-time system, Tian et al. (2021) applied modified repetitive control to improve ADRC, resulting in enhanced disturbance suppression performance in permanent magnet synchronous motor (PMSM) drives. In a minimum-phase system, Astolfi et al. (2021) used modified repetitive control to achieve a forward loop

in the control system. For PMSMs, Zheng et al. (2021) introduced a phase-advanced repetitive controller to tackle the challenges posed by various uncertainties. Focusing on system frequency, Ye et al. (2021) proposed an adaptive modified repetitive controller to achieve high-accuracy control in grid-connected inverters. This method effectively mitigates system fluctuations caused by external periodic disturbances.

However, most of the existing methods for disturbance suppression have focused on the overall performance of the control system (Zhou X et al., 2022), making it challenging to achieve exceptional disturbance suppression capabilities for periodic harmonic disturbances or narrow-band peak disturbances that occur at specific frequency points. The integration of a repetitive control strategy with a partial control method has partially addressed the issue of periodic frequency. However, these control structures are limited in that they can track or suppress the disturbance signal only for a single group of harmonic periodic frequencies. As the application environments for electro-optical tracking systems grow increasingly complex, the variety and complexity of disturbances encountered are escalating. In the context of shipboard and airborne electro-optical systems, encountering multiple sets of harmonic disturbances with different frequencies or non-periodic relationships of disturbance signals is quite common. To achieve more complex disturbance suppression, it is essential to establish a control structure that can not only ensure the basic stability of control performance across the entire frequency spectrum, but also offer flexibility in selecting disturbance suppression structures at multiple frequencies.

This paper introduces an error-based observer structure grounded in a repetitive control strategy. This structure is designed to meet the stability requirements of the control system while effectively suppressing periodic disturbances. The principal contributions of this work are as follows:

1. Considering the complex disturbance scenario in electro-optical tracking systems, an error-based observer improved by a repetitive control strategy (RCEOB) is introduced. This approach is capable of suppressing multi-period and harmonic wave disturbances within the control system.

2. Addressing the issue of signal amplification at non-notch frequencies inherent in traditional repetitive control, the filter within the repetitive controller is strategically designed to mitigate the waterbed effect to a significant extent.

3. To tackle the challenge of multi-harmonic periodic disturbance suppression, the observer structure is refined through a repetitive control strategy, enabling the suppression of harmonic periodic disturbances.

4. Guidance on parameter selection and demonstration of RCEOB's stability and robustness in practical applications are provided, offering valuable insights for engineering implementations.

2 Problem formulation

In the electro-optical tracking system depicted in Fig. 1, maintaining the tracking target at the center of the charge-coupled device (CCD) target surface requires continuous control based on the feedback error. As technology advances, electro-optical tracking systems mounted on mobile platforms are increasingly exposed to complex and variable external disturbances. These disturbances can impact various aspects of the system and ultimately affect the system output, which potentially results in tracking errors or even deviation from the target.

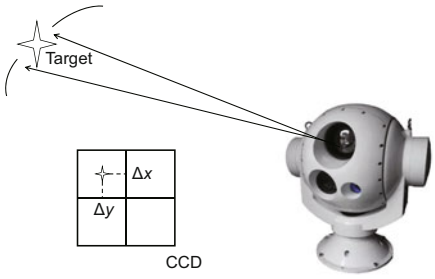

Fig. 1 Schematic of the electro-optical tracking system

The mathematical expression of system disturbance d in the case of complex disturbance is given below:

$$d(t) = \sum_{i=1}^{n} d_{\mathrm{P}i}(t) + \sum_{j=1}^{m} d_{\mathrm{A}j}(t), \tag{1}$$

where n and m represent the numbers of periodic disturbances and non-periodic disturbances, respectively. It can be seen that periodic disturbance d_{P} and non-periodic disturbance d_{A} are included. However, non-periodic disturbance usually exists in different forms of differentiation in different working

environments, which is difficult to describe by general rule methods and needs to be analyzed in combination with different actual conditions. Periodic disturbance is the form of disturbance that this study focuses on. Eq. (2) gives the specific form of the periodic disturbance, where A, ω, and φ represent the amplitude, frequency, and phase of the periodic disturbance, respectively.

$$\sum_{i=1}^{n} d_{\mathrm{P}i}(t) = \sum_{i=1}^{n} A_i \sin(\omega_i t + \varphi_i). \tag{2}$$

To address the issue of disturbance suppression in electro-optical systems, the DOB structure is commonly employed within the control systems. DOB serves as a control structure capable of observing disturbance signals. However, DOB has inherent limitations. To overcome these limitations and enhance the performance of the control structure, a Youla–Kucera parameterized error observer (EOB) method was proposed (Niu et al., 2019), as depicted in Fig. 2. This structure not only meets the disturbance suppression requirements of the control system, but also enhances the system's tracking capability.

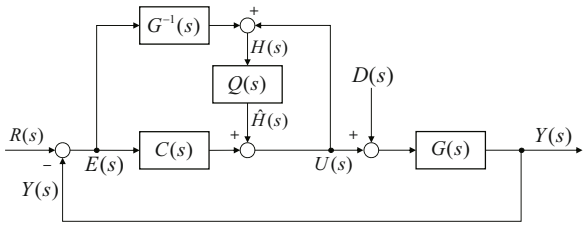

Fig. 2 Error-based observer structure

The multi-degree-of-freedom control algorithm is implemented in the proposed EOB structure, and both perturbation and tracking performances are improved. However, for the electro-optical tracking system mounted on the mobile platform, the disturbed environment is no longer a simple single-peak or single-period form. To improve the performance of EOB structures, it is necessary to improve the disturbance suppression ability of the system.

Considering the $\sum_{i=1}^{n} A_i \sin(\omega_i t + \varphi_i)$ in perturbation Eq. (2), when $n = 1$, regardless of the values of A and ω, the periodic perturbation in this single case can be suppressed by most control methods. When $n > 1$, and ω_i appears in the form of frequency doubling, some algorithms improved by repetitive control strategies can deal with this situation. However, when $n > 1$, ω_i appears in the form of harmonics at multiple groups of periods or base frequencies, and A_i exists which is far greater than the existing disturbance suppression capability of the system, it is difficult for existing control methods to deal with these more complex periodic disturbances and disturbances in the form of narrow-band peaks. To maintain the working stability and disturbance suppression capability of the electro-optical tracking system under such disturbance conditions, it is necessary for the control algorithm to have a better disturbance suppression ability at a specific frequency point, and to be able to deal with multiple groups of harmonic disturbances at different fundamental frequencies.

3 Composite control structure

3.1 Composite structure

It is evident from the analysis in Section 2 that to continue using the EOB algorithm to meet the operational requirements of the electro-optical tracking system on a mobile platform, we need to address the issue of multi-periodic disturbance while retaining the structural characteristics of EOB. In this study, we propose an enhancement to EOB using a repetitive control strategy, RCEOB. This approach aims to maximize the preservation of EOB performance while addressing the challenge of multi-periodic disturbance. Fig. 3 gives the overall block diagram of the composite control structure. The tracking transfer function (TTF), error attenuation function (EAF), and disturbance suppression function (DSF) are provided herein:

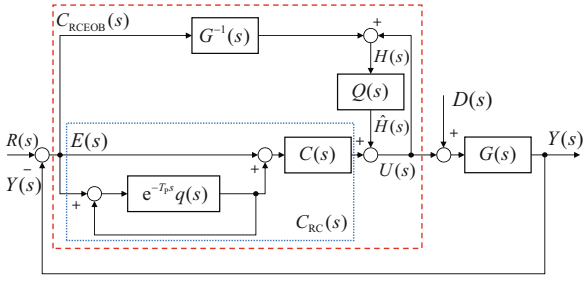

Fig. 3 Structure of the proposed error-based observer improved by a repetitive control strategy (RCEOB)

$$\begin{cases}\mathrm{TTF}_{\mathrm{RCEOB}}(s)=\dfrac{Y(s)}{R(s)}\\ =\dfrac{C_{\mathrm{RC}}(s)G(s)+G(s)G^{-1}(s)Q(s)}{1+C_{\mathrm{RC}}(s)G(s)+G(s)G^{-1}(s)Q(s)-Q(s)},\\ \mathrm{EAF}_{\mathrm{RCEOB}}(s)=\dfrac{E(s)}{R(s)}\\ =\dfrac{1-Q(s)}{1+C_{\mathrm{RC}}(s)G(s)+G(s)G^{-1}(s)Q(s)-Q(s)},\\ \mathrm{DSF}_{\mathrm{RCEOB}}(s)=\dfrac{Y(s)}{D(s)}\\ =\dfrac{G(s)-G(s)Q(s)}{1+C_{\mathrm{RC}}(s)G(s)+G(s)G^{-1}(s)Q(s)-Q(s)},\end{cases}\tag{3}$$

where R is the system input, Y is the system output, D is the disturbance input of the system, C is the controller, G is the model of the controlled object, and G^{-1} is the nominal inverse model of the controlled object. To distinguish between these two different filters, $q(s)$ is designated for the filter in the repetitive controller, while $Q(s)$ represents the EOB filter. For simplicity, the $C_{\mathrm{RC}}(s)$ structure within the dotted-line block is not fully elaborated upon. The complete form is as given in Eq. (4). Detailed analysis can be found in Section 3.2.2.

$$C_{\mathrm{RC}}(s)=\frac{C(s)}{1-\mathrm{e}^{-T_{\mathrm{P}}s}q(s)}.\tag{4}$$

Then the stability and robustness of RCEOB are analyzed.

Theorem 1 (Stability) In the case where the closed-loop controller $C(s)$ is stable, the following requirements are made for the $Q(s)$ and $q(s)$ filter structures in the control structure. When the following expression is met, the RCEOB structure is stable:

$$\left\|\frac{\mathrm{e}^{-T_{\mathrm{P}}s}q(s)C(s)-\left(1-\mathrm{e}^{-T_{\mathrm{P}}s}q(s)\right)\left(C(s)Q(s)+G^{-1}(s)Q(s)\right)}{(1+C(s)G(s))\left[C(s)+G^{-1}(s)Q(s)\left(1-\mathrm{e}^{-T_{\mathrm{P}}s}q(s)\right)\right]}\right\|_{\infty}<1.\tag{5}$$

The proof of Theorem 1 is provided in the supplementary materials.

Theorem 2 (Robust stability) In the RCEOB control system, if the RCEOB structure is stable, and if there is a small disturbance $\Delta(s)$ in the control object $G(s)$, which satisfies

$$G_{\mathrm{P}}(s)=G(s)(1+\Delta(s)),\tag{6}$$

where $\Delta(s)$ represents the modeling uncertainty, which denotes the system's internal disturbance, and $\Delta(s)$ is stable and bounded, the given system has robust stability if the following expression is true:

$$\|\Delta(s)\mathrm{TTF}_{\mathrm{RCEOB}}(s)\|_{\infty}<1.\tag{7}$$

The proof of Theorem 2 is provided in the supplementary materials.

Remark 1 Theorem 2 guarantees that the control system can maintain overall stability in the case of small perturbations in the object model.

3.2 Notch structure analysis

After the stability and robustness analysis is completed, the controller and filter in the control structure are described. After analyzing the function and improvement of each structure, the suppression performance of the control structure under the influence of frequency incoherence and multiple frequency multiplier harmonic disturbances is described.

3.2.1 Notch at single and discrete frequency points

The notch effect at discrete frequency points in the RCEOB structure is realized by the improved structure of $Q(s)$. The specific structure is given below:

$$Q_{\mathrm{N}}(s)=1-\prod_{i=1}^{a}\frac{s^2+\eta_i\omega_i s+\omega_i^2}{s^2+\alpha_i\eta_i\omega_i s+\omega_i^2}\left(1-q_{\mathrm{LPF}}(s)\right).\tag{8}$$

$Q_{\mathrm{N}}(s)$ corresponds to multiple filters with different cycle frequencies, $q_{\mathrm{LPF}}(s)$ is a low-pass filter to ensure the stability of the structure (here to highlight the characteristics of the structure, a first-order low-pass filter is used by default), ω_i is the center frequency of the i^{th} notch structure, and α_i and η_i are structural parameters, which are detailed in Section 3.4.

Theorem 3 For $Q_{\mathrm{N}}(s)$, when $a=1$, the complementary sensitivity function $\mathrm{CSF}_{Q_{\mathrm{N}}}(s)$ is at ω_1, and $\exists\delta>0,\delta\to0$ exists to make $\mathrm{CSF}_{Q_{\mathrm{N}}}(\omega_1)\ll\mathrm{CSF}_{Q_{\mathrm{N}}}(\omega_1+\delta)\mathrm{CSF}_{Q_{\mathrm{N}}}(\omega_1)\ll\mathrm{CSF}_{Q_{\mathrm{N}}}(\omega_1-\delta)$ true.

The proof of Theorem 3 is provided in the supplementary materials.

Remark 2 Theorem 3 states that for $Q_{\mathrm{N}}(s)$, good notch effect at ω_1 can be achieved.

Combined with the curve of the complementary sensitivity function, the frequency of the filter notch point is set to 0.5 Hz for easy observation. Fig. 4 confirms the theoretical analysis.

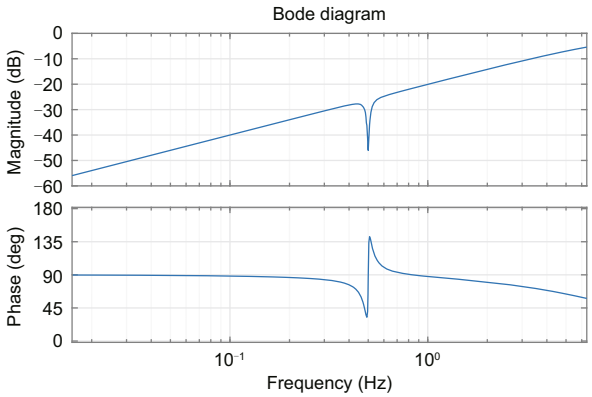

Fig. 4 The complementary sensitivity function of Q_{N} when $a=1$, $\alpha_1=10$, $\eta_1=0.01$, $\omega_1=\pi$ Hz

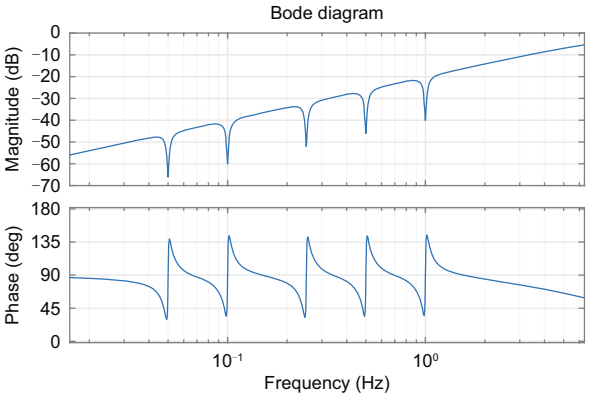

Fig. 5 The complementary sensitivity function of Q_{N} when $a=5$, $\alpha_1=\alpha_2=\alpha_3=\alpha_4=\alpha_5=10$, $\eta_1=\eta_2=\eta_3=\eta_4=\eta_5=0.01$, $\omega_1=0.1\pi$ Hz, $\omega_2=0.2\pi$ Hz, $\omega_3=0.5\pi$ Hz, $\omega_4=\pi$ Hz, $\omega_5=2\pi$ Hz

Theorem 4 For $Q_{\mathrm{N}}(s)$, when $a\neq 1$, the complementary sensitivity function $\mathrm{CSF}_{Q_{\mathrm{N}}}(s)$ is at ω_i $(i\in[1,a])$, and $\exists\delta>0,\delta\to 0$ exists to make $\mathrm{CSF}_{Q_{\mathrm{N}}}(\omega_i)\ll\mathrm{CSF}_{Q_{\mathrm{N}}}(\omega_i+\delta)\mathrm{CSF}_{Q_{\mathrm{N}}}(\omega_i)\ll\mathrm{CSF}_{Q_{\mathrm{N}}}(\omega_i-\delta)$ true.

The proof of Theorem 4 is provided in the supplementary materials.

Remark 3 Theorem 4 states that the above $Q_{\mathrm{N}}(s)$ filter structure can be implemented simultaneously at multiple notch points.

At $\omega_1,\omega_2,...,\omega_a$, the frequency response of the filter reaches the minimum value. At the same time, the frequency response keeps monotonically increasing between different notch points until the next notch point takes the minimum again. Therefore, the filter structure can be extended from a single frequency to multiple notch frequency points, and even realize multiple specific frequency notches with discrete periodic frequencies. In this case, the curve of the complementary sensitivity function of the trapping structure is given.

The reliability of Theorem 4 can be verified by the complementary sensitivity function of Q_{N} as shown in Fig. 5.

Theorems 3 and 4 show how the RCEOB structure realizes the notch of the control structure at a single frequency point and discrete frequency points, respectively. In addition, the complex disturbance environment must contain harmonic disturbances in the form of periodic frequencies.

3.2.2 Notch at the harmonic periodic frequency

In the RCEOB structure, there are two structures that can realize the notch at the harmonic periodic frequency, namely the repetitive controller and the EOB filter structure.

1. Repetitive controller

The specific control structure of the repetitive controller is shown in Fig. 6. By using this structure, the closed-loop controller can achieve high performance and suppress harmonic signal disturbance at the repetition frequency.

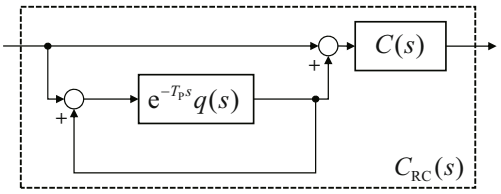

Fig. 6 Repetitive control structure

In Eq. (4), $1-\mathrm{e}^{-T_{\mathrm{P}}s}q(s)$ provides the theoretical limit gain at the harmonic frequency based on the fundamental frequency $1/T_{\mathrm{P}}$ and the integer multiple of the fundamental frequency, and $q(s)$ in the classical repetitive control structure is a low-pass filter, so that the controller as a whole can have better disturbance immunity in the main operating frequency band.

As can be seen from Fig. 7, as a classical control method, repetitive control has excellent disturbance suppression performance under the disturbance input scenarios of repetition frequency. However, according to Bird's integral theorem (Zhang and Sun, 2003), the continuous theory method completely avoids the amplification effect at other non-trapping frequencies caused by the waterbed effect, and such comb effect will lead to disturbance

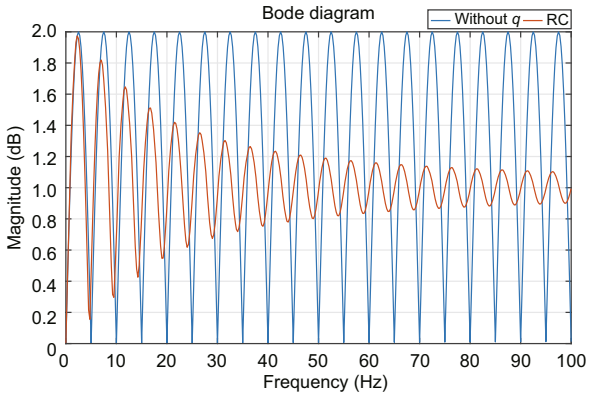

Fig. 7 Comparison between the sensitivity function of $1-\mathrm{e}^{-T_\mathrm{P}s}$ and the effect of $1-\mathrm{e}^{-T_\mathrm{P}s}q(s)$, where T_P is the reciprocal of the base frequency $f=5$ Hz and the system sampling frequency $f_\mathrm{s}=200$ Hz. References to color refer to the online version of this figure

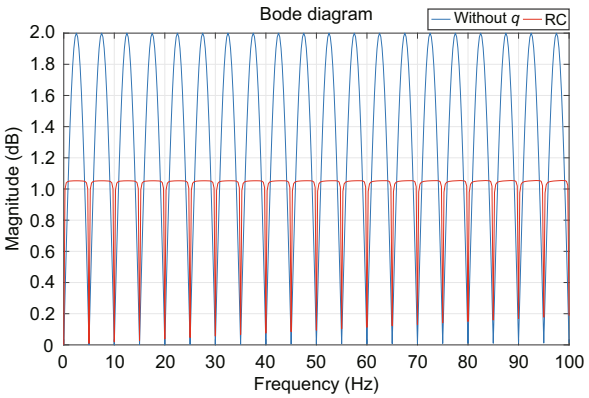

Fig. 8 When $k=0.3$, comparing the effect of $1-\mathrm{e}^{-T_\mathrm{P}s}$ and the improved sensitivity function of $1-\mathrm{e}^{-T_\mathrm{P}s}q(s)$, where T_P is the reciprocal of the fundamental frequency $f=5$ Hz and the system sampling frequency $f_\mathrm{s}=200$ Hz. References to color refer to the online version of this figure

amplification at $\omega_i \neq i/T_\mathrm{P}, i \in \mathbb{N}_+$. It may also cause the notch frequency point to be inaccurate.

To suppress the waterbed effect, the $q(s)$ in the repetitive controller is improved as follows:

$$q_\mathrm{new}(s)=\frac{kq(s)}{1-(1-k)\mathrm{e}^{-T_\mathrm{P}s}},\quad k\in(0,1), \tag{9}$$

where k is the structural parameter and T_P influences the notch frequency.

Theorem 5 When $q(s)=q_\mathrm{new}(s)$ is satisfied in the repetitive controller, the sensitivity function value can be made to approach 1 at the non-notch frequency, that is, $\omega_i \neq i/T_\mathrm{P}$, $i\in\mathbb{N}_+$.

Remark 4 Theorem 5 states that the improved filter can effectively suppress the waterbed effect and reduce the frequency amplification at non-notch points.

The proof of Theorem 5 is provided in the supplementary materials.

Note that the improved repetitive controller suppresses the waterbed effect and realizes the suppression effect of recurring harmonic disturbances.

Fig. 8 shows that, taking the fundamental frequency $f=5$ Hz as an example, the disturbance amplification effect at the non-notch frequency is significantly reduced, and the amplification effect on the disturbance is only 1.05 times, with a decrease of 47.5%.

2. Filter improved by repetitive control strategy

By improving the $q(s)$ filter structure in the controller, a group of harmonic disturbances with the fundamental frequency and its frequency doubling can be solved. In the control process of the electro-optical tracking system, there may be a group of harmonics and a single fundamental wave, or even multiple groups of harmonic disturbances. Next, we propose another improvement and theoretical analysis of the $Q(s)$ structure. By introducing the repetitive control strategy into the EOB filter structure, we try to expand the disturbance suppression ability of the control structure in the above working environment.

The specific structure of the improved filter is given below:

$$Q_\mathrm{RC}(s)=[1-\beta(1-\mathrm{e}^{-T'_\mathrm{P}s})]\cdot q_\mathrm{LPF}(s), \tag{10}$$

where $Q_\mathrm{RC}(s)$ introduces the idea of repetitive controller into the filter structure and achieves the suppression of harmonic disturbance in the filter. β is the structural parameter, which is analyzed in detail in Section 3.4.

At the same time, $Q_\mathrm{RC}(s)$ is independent of the repetitive control structure in the controller. To distinguish the parameters in the repetitive controller, T'_P is used; $q_\mathrm{LPF}(s)$ is a low-pass filter to ensure the stability of the structure, and a first-order low-pass filter is used here.

Lemma 1 For $Q_\mathrm{RC}(s)=[1-\beta(1-\mathrm{e}^{-T'_\mathrm{P}s})]\cdot q_\mathrm{LPF}(s)$, it can realize the notch at the repetition frequency in the EOB filter structure.

As for $Q_\mathrm{RC}(s)=[1-\beta(1-\mathrm{e}^{-T'_\mathrm{P}s})]\cdot q_\mathrm{LPF}(s)$, it has a simpler structure and fewer parameters than $Q_\mathrm{N}(s)$. The principle of $Q_\mathrm{RC}(s)$ is then analyzed.

By observing the structure of the filter, it can be seen that the improved structure is based on the original low-pass filter structure by adding a structure similar to traditional repetitive control.

Similar to the repetitive controller, the repetitive control modified filter uses the structure of $1-\mathrm{e}^{-T_{\mathrm{P}}' s}$ to achieve high performance at the fundamental frequency and its integer multiples.

Remark 5 The changes proposed in Lemma 1 give the EOB structure the ability to handle a set of harmonic disturbances independently.

According to the curves of the sensitivity function and the complementary sensitivity function in Fig. 9, it can be seen that the filter $Q_{\mathrm{RC}}(s)$ improved by repetitive control can easily suppress the disturbance when ω_i is a group of harmonics in periodic disturbance, while ensuring the stability of the overall control structure.

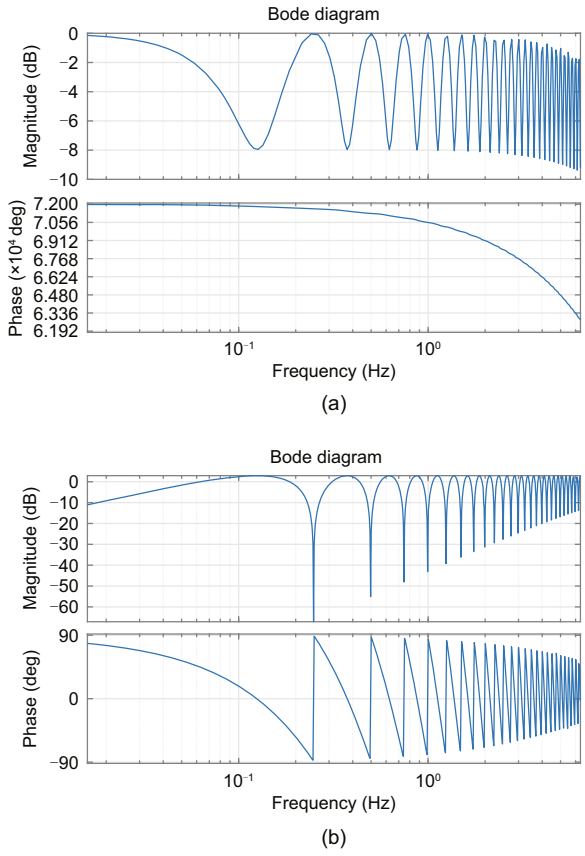

Fig. 9 Sensitivity function curve of $Q_{\mathrm{RC}}(s)$ (a) and complementary sensitivity function curve of $1-Q_{\mathrm{RC}}(s)$ (b)

3.3 Implementation of the multi-notch structure

After the analysis of the control structure, this subsection will focus on the analysis of how to use the composite control structure to realize a multi-notch structure, so as to achieve disturbance suppression of periodic harmonics and non-harmonic discrete periodic disturbances at multiple frequency points.

In Section 3.1, the complete control structure of RCEOB is given. To analyze how this structure implements multiple notches, the part before the control object $G(s)$ is now regarded as an overall controller, which is shown in the dashed-line box in Fig. 3.

According to Eq. (9), the transfer function of the composite controller is given by

$$\begin{aligned} C_{\mathrm{RCEOB}} &= \frac{C_{\mathrm{RC}}(s)+G^{-1}(s)Q(s)}{1-Q(s)} \\ &= \frac{C(s)+G^{-1}(s)Q(s)(1-\mathrm{e}^{-T_{\mathrm{P}}s}q(s))}{(1-\mathrm{e}^{-T_{\mathrm{P}}s}q(s))(1-Q(s))}. \end{aligned} \tag{11}$$

The denominator of the controller is analyzed using the same analysis method as that for the repetitive controller:

$$\mathrm{den}_{C_{\mathrm{RCEOB}}} = (1-\mathrm{e}^{-T_{\mathrm{P}}s}q(s))(1-Q(s)). \tag{12}$$

Lemma 2 When $q(s)$ and $Q(s)$ given in Eqs. (11) and (12) are $q_{\mathrm{new}}(s)$ and $Q_{\mathrm{N}}(s)$ as given in Section 3.2 respectively, simultaneous trapping at discrete frequency points and single-harmonic periodic frequency points can be achieved.

The two factors in Eq. (12) correspond exactly to $1-\mathrm{e}^{-T_{\mathrm{P}}s}q(s)$ of the repetitive controller that generates the harmonic theoretical limit gain and to the complementary sensitivity function $\mathrm{CSF}_Q = 1-Q(s)$ of the filter structure in EOB. This structure can realize the notch effect of the two structures analyzed before. First, on the basis of repeating the notch at one cycle frequency of the controller, $Q_{\mathrm{N}}(s)$ is added to realize the effect of increasing the number of discrete notch points.

Fig. 10 shows the control effect of the repetitive controller and $Q_{\mathrm{N}}(s)$ acting simultaneously in the main operating frequency band.

It can be seen that by adjusting the filter structure, the composite control structure can achieve the notch effect for multiple cycles.

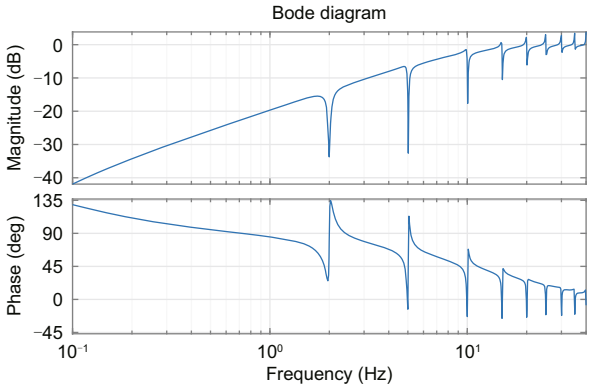

Fig. 10 The sensitivity function curve of $(1-\mathrm{e}^{-T_{\mathrm{P}}s}q(s))(1-Q_{\mathrm{N}}(s))$ in the composite control structure when the frequencies of the notch points are set to 5 Hz and its frequency doubling in a repetitive controller, and to 1 Hz and 7 Hz in $Q_{\mathrm{N}}(s)$

Remark 6 Lemma 2 shows that the composite control structure can realize disturbance suppression of the harmonic periodic frequency and discrete frequency point periodic disturbance simultaneously.

Note that $Q_{\mathrm{N}}(s)$ at this point is under the condition $a=2$. In combination with the analysis of stability conditions given in Eq. (5), it can be seen that the increase of the value of a will gradually increase the complexity of the multiplicative part of the filter structure, which will definitely lead to the failure of the control system to meet the stability conditions. In other words, the composite structure with $Q_{\mathrm{N}}(s)$ can indeed improve the disturbance suppression performance when dealing with a set of periodic frequency doubling harmonics and a few discrete frequency disturbances. However, when the second group of periodic frequency doubling harmonic disturbances occur, to ensure the stability of the system, this structure can cover the disturbance signal only at the low-frequency narrow-band peak. It is not possible to suppress the periodic frequency doubling harmonic disturbances in all operating frequency domains.

Lemma 3 When $q(s)$ and $Q(s)$ given in Eqs. (11) and (12) are $q_{\mathrm{new}}(s)$ and $Q_{\mathrm{RC}}(s)$ as given in Section 3.2 respectively, simultaneous trapping at multi-harmonic periodic frequency points can be achieved.

The improved $Q_{\mathrm{RC}}(s)$ combined with the repetitive control strategy can deal with the situation where there are two groups of periodic harmonic disturbances at the same time, in which case Eq. (12) becomes

$$\mathrm{den}_{C_{\mathrm{RCEOB}}}=(1-\mathrm{e}^{-T_{\mathrm{P}}s}q(s))(1-Q_{\mathrm{RC}}(s)). \quad (13)$$

At this point, another factor in Eq. (13) becomes the complementary sensitivity function of $Q_{\mathrm{RC}}(s)$. The two factors in the structure have repetitive control structures and independent parameters, which means that the compound control structure can realize the notch at two groups of periodic frequency doubling harmonic points at the same time. Compared with $Q_{\mathrm{N}}(s)$ with a larger a, the overall structure of the $Q_{\mathrm{RC}}(s)$ controller is simple, and it is easy to meet the stability condition given by Theorem 1, which ensures the stability of the overall control structure.

As can be seen from Fig. 11, the composite controller at this time completes the notch at two groups of harmonic frequencies, i.e., 1, 2, 3, ... Hz and 5, 10, 15, ... Hz.

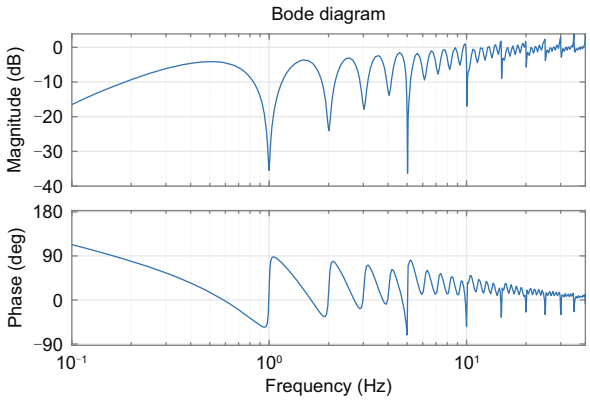

Fig. 11 The sensitivity function curve of $(1-\mathrm{e}^{-T_{\mathrm{P}}s}q(s))(1-Q_{\mathrm{RC}}(s))$ in the composite control structure when the frequencies of the notch points are set to 5 Hz and its frequency doubling in a repetitive controller, and to 1 Hz and its frequency doubling in $Q_{\mathrm{RC}}(s)$

Remark 7 Lemma 3 shows that the complex control structure can suppress multiple independent harmonic periodic frequency disturbances simultaneously.

To sum up, the composite control structure given by Eq. (11) can realize multiple notch waves. At the same time, with different $Q(s)$, the structure can realize notch waves for single periodic harmonics, narrow-band peak disturbance at discrete frequencies, and two independent periodic harmonics separately, to meet the disturbance suppression requirements of an actual electro-optical system in different situations.

3.4 Parameter selection for the multi-notch structure

After introducing how the composite control structure achieves multi-notch effect, this subsection focuses on the selection of parameters in the composite controller, and finally gives a group of references for the selection of filter parameters in the multi-notch structure.

Table 1 lists all the adjustable parameters in the $q(s)$ and two $Q(s)$ structures. For the repetitive controller, the main adjustable parameter is k, and the influence of different k values on the control effect at a fixed base frequency is compared (Fig. 12).

Table 1 All adjustable parameters in the composite controller

Source	Parameter
$C_{\mathrm{RC}}(s)$	k
	T_{P}
$Q_{\mathrm{N}}(s)$	α_i
	η_i
	ω_i
$Q_{\mathrm{RC}}(s)$	β
	T'_{P}

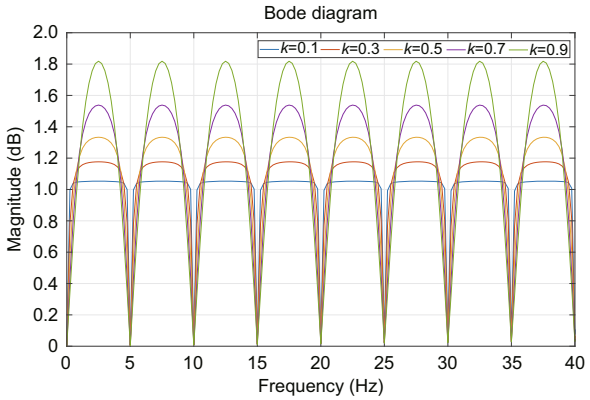

Fig. 12 Comparison of the sensitivity functions of $1-\mathrm{e}^{-T_{\mathrm{P}}s}q(s)$ when k takes different values. The base frequency is $f=5$ Hz $=1/T_{\mathrm{P}}$, and the sampling frequency is 100 Hz. References to color refer to the online version of this figure

By comparison, it can be seen that the value of $k\in(0,1)$ significantly influences the waterbed effect of the filter in the repetitive control structure. The smaller the value of k is, the more obvious the suppression effect on the error amplification at the non-notch frequencies will be, while the notch effect on the fundamental and harmonic frequencies will not be affected.

In $Q_{\mathrm{N}}(s)$, there are three adjustable parameters, among which one is the frequency at the i^{th} single notch. In the case of a fixed ω_i, the influence of the value ranges of two other structural parameters on the overall effect of the filter is compared, where $\alpha_i>1$ must be ensured.

First, analyze the influence of α_i on the filter effect. Through theoretical analysis, it can be seen that α_i affects mainly the peak depth of the notch point in the notch structure of the filter. A larger value of α_i can provide better notch effect at the set frequency, but it will also change the system characteristics at the surrounding frequency (Fig. 13).

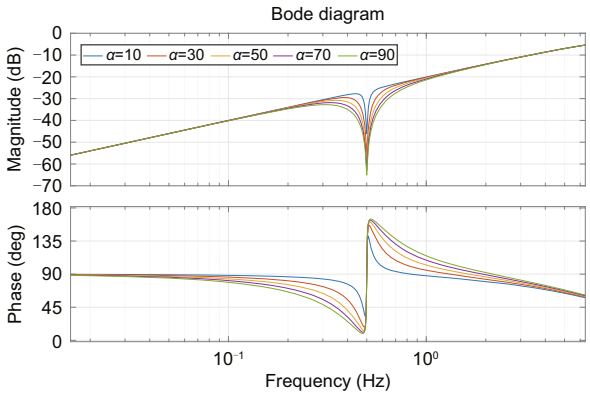

Fig. 13 Changes of the complementary sensitivity function of $Q_{\mathrm{N}}(s)$ with different α values. The sampling frequency is 100 Hz, the notch frequency is $\omega=5$ Hz, and the other structural parameter η is fixed as 0.01. References to color refer to the online version of this figure

For the other structural parameter η_i, it can be seen from the comparison that η_i does not affect the notch depth at the trapping point, but acts only on the waveform around the trapping point. The smaller the value of η_i is, the more concentrated the trapping effect will be, and the less the effect will be at non-trapping frequencies (Fig. 14).

To sum up, for $Q_{\mathrm{N}}(s)$, on the premise of meeting the response stability and robustness, for each notch point $\omega_i, i=1,2,...,a$, α_i should be as large as possible, and η_i should be as small as possible, so as to realize the notch effect at the set frequency points relatively concentrated.

For $Q_{\mathrm{RC}}(s)$ with improved repetitive control, except for setting the notch frequency, there is only one adjustable parameter β.

β has a complex influence on the performance

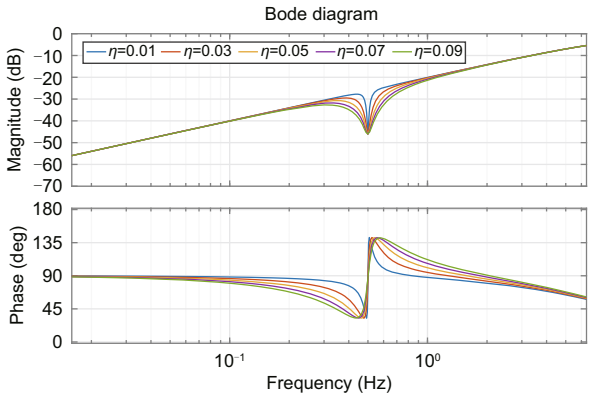

Fig. 14 Changes of the complementary sensitivity function of $Q_{\mathrm{N}}(s)$ with different values of η. The sampling frequency is 100 Hz, the notch frequency is $\omega = 5$ Hz, and the other structural parameter α is fixed as 10. References to color refer to the online version of this figure

of $Q_{\mathrm{RC}}(s)$. As shown in Fig. 15, the increase of β leads to much better notch performance, but it may cause waterbed effect at other non-notch frequencies to amplify the disturbance. According to Bird's integral theorem, this property is consistent with the characteristics of repetitive control. At the same time, a too small β value may lead to an inaccurate frequency at the trapping point, which will influence the disturbance suppression effect.

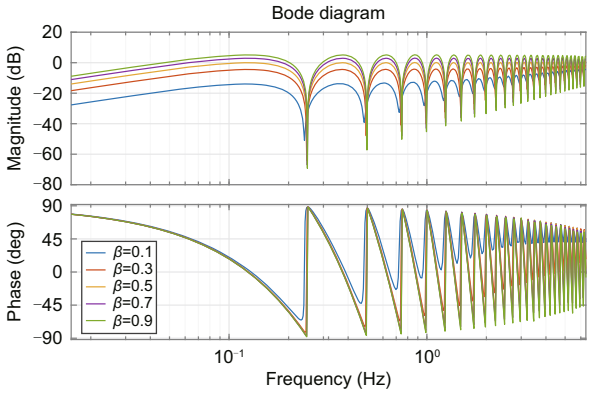

Fig. 15 Comparison of the complementary sensitivity function of $Q_{\mathrm{RC}}(s)$ with different values of β. The sampling frequency is 100 Hz and the notch base frequency is 0.25 Hz. References to color refer to the online version of this figure

Finally, the reference value of each parameter is analyzed in this subsection (Table 2), and the actual effects of multiple notches under the modified reference values are given (Fig. 16).

Table 2 All adjustable parameters in the composite controller (with value)

Source	Parameter	Value
$C_{\mathrm{RC}}(s)$	k	0.1
	T_{P}	0.2 s
$Q_{\mathrm{N}}(s)$	α_i	10
	η_i	0.01
	ω_i	2 Hz
$Q_{\mathrm{RC}}(s)$	β	0.5
	T'_{P}	1 s

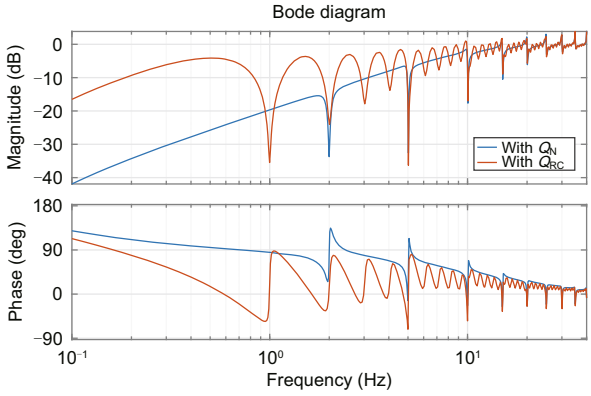

Fig. 16 The sensitivity function of $(1-\mathrm{e}^{-T_{\mathrm{P}}s}q(s))(1-Q(s))$ in the composite controller structure under the parameters given in Table 2. References to color refer to the online version of this figure

4 Experimental verification

4.1 Experimental platform construction

To verify the effectiveness of the method, a system is built as shown in Fig. 17.

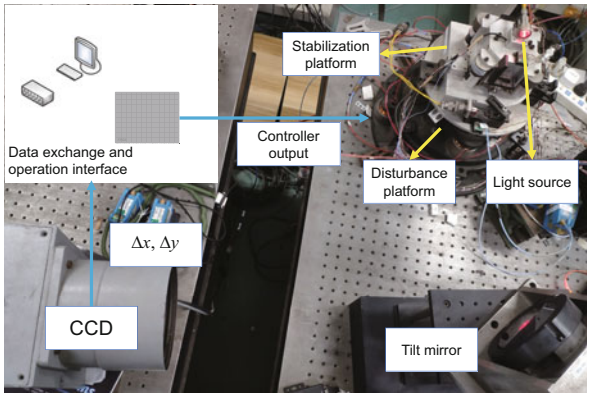

Fig. 17 Composition of the experimental platform

Based on the platform, the controlled object is fitted first, and the controller in the control structure is set according to the fitting results to ensure the stability of the single closed-loop process.

Through open-loop measurement, it can be seen that in the main operating frequency band 0–50 Hz, the control object can be regarded as a linear object (Fig. 18), and a second-order oscillation link is used to fit it:

$$G(s)=\frac{12\ 320}{37.7s^2+619.7s+53\ 580}. \tag{14}$$

Based on the fitting results, to ensure the stability of the system, the multi-notch effect of the composite controller is mainly tested, and a simple controller $C(s)$ is designed:

$$C(s)=\frac{9425s^2+154\ 900s+13\ 390\ 000}{142.1s^2+53\ 580s}. \tag{15}$$

4.2 Closed-loop experimental results

To verify the effectiveness of the method and show the performance improvement of the RCEOB method at the trapping point, the actual transfer functions, error-tracking functions, and disturbance suppression functions of different methods are measured, and the experimental results are given in the form of Bode diagram (Fig. 19). Refer to Table 2 for RCEOB structure parameters.

The analysis of experimental results is provided in the supplementary materials.

4.3 Single-frequency disturbance

The experimental results are provided in the supplementary materials.

4.4 Multi-frequency disturbance

The experimental results are provided in the supplementary materials.

5 Conclusions

In this paper, a multi-notch controller structure (RCEOB) with multiple selectable parameters is proposed to deal with periodic disturbance in the process of the electro-optical tracking system, especially multi-periodic harmonics and narrow-band peak disturbances, which are difficult to suppress by the existing disturbance suppression methods. The RCEOB structure is proposed to suppress the disturbance on the premise of ensuring the stability of the system, and the filter in the structure is improved by a repetitive control strategy, which achieves disturbance suppression in the case of complex disturbance. In addition, parameter selection for the composite structure is analyzed, and multi-notch disturbance suppression is realized. Finally, an experimental platform is set up to verify the effectiveness of the control method and the disturbance suppression performance, proving that the proposed method has excellent performance with respect to theoretical analysis.

However, according to Bird's integral theorem, the waterbed effect must exist in any repetitive controller or filter improved by the repetitive control strategy, which is completely eliminated by the theory. How to further suppress the waterbed effect is a direction of future thinking. At the same time, the existence of the multi-notch structure may affect the accuracy of each notch structure, and how to improve the structure to make each notch point more accurate is another problem to be solved.

The follow-up work plan is based on the multi-degree-of-freedom control structure, combined with the adaptive recognition process, striving to realize the disturbance suppression algorithm with self-adjusting ability.

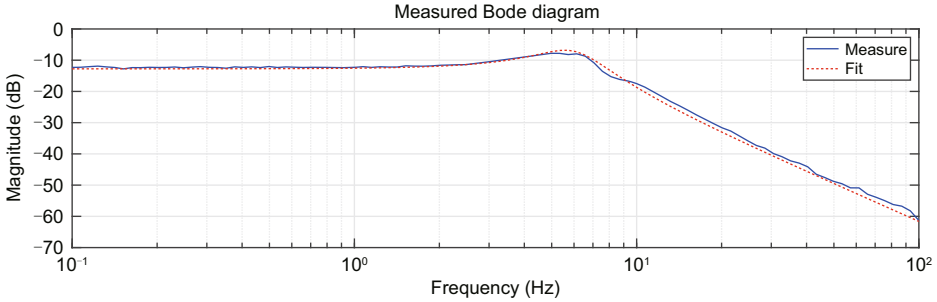

Fig. 18 Fitting of open-loop characteristics of experimental subjects

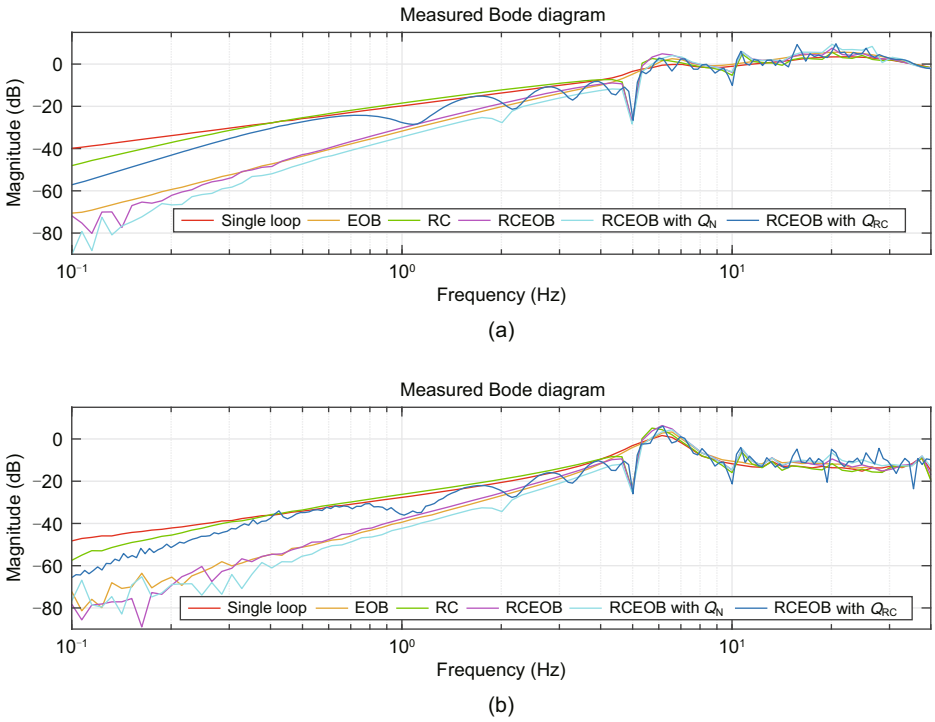

Fig. 19 Comparison of error-tracking performance (a) and disturbance suppression performance (b) of different control methods on the experimental platform. References to color refer to the online version of this figure

Contributors

Mai TANG and Yao MAO designed the research. Mai TANG and Wenqiang XIA processed the data. Mai TANG drafted the paper. Wenqiang XIA and Jiuqiang DENG helped organize the paper. Mai TANG and Jiuqiang DENG revised and finalized the paper.

Conflict of interest

All the authors declare that they have no conflict of interest.

Data availability

The data that support the findings of this study are available from the corresponding author upon reasonable request.

References

Astolfi D, Marx S, van de Wouw N, 2021. Repetitive control design based on forwarding for nonlinear minimum-phase systems. *Automatica*, 129:109671. https://doi.org/10.1016/j.automatica.2021.109671

Beaulieu-Laroche L, Brown NJ, Hansen M, et al., 2021. Allometric rules for Mammalian cortical layer 5 neuron biophysics. *Nature*, 600(7888):274-278. https://doi.org/10.1038/s41586-021-04072-3

Berkefeld T, Soltau D, Schmidt D, et al., 2010. Adaptive optics development at the German solar telescopes. *Appl Opt*, 49(31):G155-G166. https://doi.org/10.1364/AO.49.00G155

Caruso H, 2001. MIL-STD-810F, test method standard for environmental engineering considerations and laboratory tests. *J IEST*, 44(3):30-34. https://doi.org/10.17764/jiet.44.3.f45015p217843r36

Chen X, Tomizuka M, 2013. New repetitive control with improved steady-state performance and accelerated transient. *IEEE Trans Contr Syst Technol*, 22(2):664-675. https://doi.org/10.1109/TCST.2013.2253102

Deng JQ, Zhou X, Mao Y, 2021. On vibration rejection of nonminimum-phase long-distance laser pointing system with compensatory disturbance observer. *Mechatronics*, 74:102490. https://doi.org/10.1016/j.mechatronics.2021.102490

Deng JQ, Xue WC, Zhou X, et al., 2022. On dual compensation to disturbances and uncertainties for inertially stabilized platforms. *Int J Contr Automat Syst*, 20(5):1521-1534. https://doi.org/10.1007/S12555-021-0022-3

Deng JQ, Xue WC, Liang W, et al., 2023. On adjustable and lossless suppression to disturbances and uncertainties for nonminimum-phase laser pointing system. *ISA Trans*, 136:727-741. https://doi.org/10.1016/j.mechatronics.2021.102490

Dong QR, Liu YK, Zhang YL, et al., 2018. Improved ADRC with ILC control of a CCD-based tracking loop for fast steering mirror system. *IEEE Photon J*, 10(4):1-14. https://doi.org/10.1109/JPHOT.2018.2846287

Downey G, Stockum L, 1989. Electro-optical tracking systems considerations. Proc SPIE 1111, Acquisition, Tracking, and Pointing III, p.70-84. https://doi.org/10.1117/12.977971

Fedele G, Ferrise A, 2014. Periodic disturbance rejection with unknown frequency and unknown plant structure. *J Franklin Inst*, 351(2):1074-1092. https://doi.org/10.1016/j.jfranklin.2013.10.013

Hara S, Yamamoto Y, Omata T, et al., 1988. Repetitive control system: a new type servo system for periodic exogenous signals. *IEEE Trans Automat Contr*, 33(7):659-668. https://doi.org/10.1109/9.1274

Inoue T, Nakano M, Kubo T, et al., 1981. High accuracy control of a proton synchrotron magnet power supply. *IFAC Proc Vol*, 14(2):3137-3142. https://doi.org/10.1016/S1474-6670(17)63938-7

Kalita A, Mrozek-McCourt M, et al., 2023. Microstructure and crystal order during freezing of supercooled water drops. *Nature*, 620(7974):557-561. https://doi.org/10.1038/s41586-023-06283-2

Kennedy PJ, Kennedy RL, 2003. Direct versus indirect line of sight (LOS) stabilization. *IEEE Trans Contr Syst Technol*, 11(1):3-15. https://doi.org/10.1109/TCST.2002.806443

Lan YH, He JL, Li P, et al., 2020. Optimal preview repetitive control with application to permanent magnet synchronous motor drive system. *J Franklin Inst*, 357(15):10194-10210. https://doi.org/10.1016/j.jfranklin.2020.04.026

Lee HS, Tomizuka M, 1996. Robust motion controller design for high-accuracy positioning systems. *IEEE Trans Ind Electron*, 43(1):48-55. https://doi.org/10.1109/41.481407

Lee JS, Lim SY, Kim I, et al., 2016. An adaptive disturbance rejection method with stability enhancement using adjustable dead zone for hard disk drives. *IEEE Trans Magn*, 53(3):1-9. https://doi.org/10.1109/TMAG.2016.2626314

Li ZJ, Mao Y, Qi B, et al., 2022. Research on control technology of single detection based on position correction in quantum optical communication. *Opto-Electron Eng*, 49(3):210311 (in Chinese). https://doi.org/10.12086/oee.2022.210311

Longman RW, 2000. Iterative learning control and repetitive control for engineering practice. *Int J Contr*, 73(10):930-954. https://doi.org/10.1080/002071700405905

Lu LL, Wang XQ, Jin LH, et al., 2024. Current optimization-based control of dual three-phase PMSM for low-frequency temperature swing reduction. *Def Technol*, 34:238-246. https://doi.org/10.1016/j.dt.2023.07.002

Madsen LS, Laudenbach F, Askarani MF, et al., 2022. Quantum computational advantage with a programmable photonic processor. *Nature*, 606(7912):75-81. https://doi.org/10.1038/s41586-022-04725-x

Nie K, Li ZJ, Guo T, et al., 2021. Improved repetitive control with model-assisted extended state observer for optoelectronic tracking system. Proc IEEE 10$^{\text{th}}$ Data Driven Control and Learning Systems Conf, p.360-366. https://doi.org/10.1109/DDCLS52934.2021.9455552

Niu SX, Yang T, Tang T, et al., 2019. Wideband vibrations rejection of tip-tilt mirror using error-based disturbance observer. *IEEE Access*, 8:5131-5138. https://doi.org/10.1109/ACCESS.2019.2962808

Ohishi K, Nakao M, Ohnishi K, et al., 1987. Microprocessor-controlled DC motor for load-insensitive position servo system. *IEEE Trans Ind Electron*, IE-34(1):44-49. https://doi.org/10.1109/TIE.1987.350923

Ren W, Luo Y, He QN, et al., 2018. Stabilization control of electro-optical tracking system with fiber-optic gyroscope based on modified Smith predictor control scheme. *IEEE Sens J*, 18(19):8172-8178. https://doi.org/10.1109/JSEN.2018.2835147

Ricks TP, Burton MM, Cruger W, et al., 2004. Stabilized electro-optical airborne instrumentation platform (SEAIP). Proc SPIE 5268, Chemical and Biological Standoff Detection, p.202-209. https://doi.org/10.1117/12.519168

Shamsuzzoha M, Lee M, 2009. Enhanced disturbance rejection for open-loop unstable process with time delay. *ISA Trans*, 48(2):237-244. https://doi.org/10.1016/j.isatra.2008.10.010

Shen XN, Liu JX, Alcaide AM, et al., 2022. Adaptive second-order sliding mode control for grid-connected NPC converters with enhanced disturbance rejection. *IEEE Trans Power Electron*, 37(1):206-220. https://doi.org/10.1109/TPEL.2021.3099844

Snigirev V, Riedhauser A, Lihachev G, et al., 2023. Ultrafast tunable lasers using lithium niobate integrated photonics. *Nature*, 615(7952):411-417. https://doi.org/10.1038/s41586-023-05724-2

Sobhy A, Lei D, 2021. Model-assisted active disturbance rejection controller for maximum efficiency schemes of DFIG-based wind turbines. *Int Trans Electr Energy Syst*, 31(11):e13107. https://doi.org/10.1002/2050-7038.13107

Somaschini R, Bianchi G, Scaccabarozzi D, et al., 2019. Characterization of commercial fast steering mirrors for space application. Proc IEEE 5$^{\text{th}}$ Int Workshop on Metrology for AeroSpace, p.468-472. https://doi.org/10.1109/MetroAeroSpace.2019.8869640

Tang T, Niu SX, Yang T, et al., 2019. Vibration rejection of tip-tilt mirror using improved repetitive control. *Mech Syst Signal Process*, 116:432-442. https://doi.org/10.1016/j.ymssp.2018.06.060

Tian MH, Wang B, Yu Y, et al., 2021. Discrete-time repetitive control-based ADRC for current loop disturbances suppression of PMSM drives. *IEEE Trans Ind Inform*, 18(5):3138-3149. https://doi.org/10.1109/TII.2021.3107635

Wang YC, Zheng LF, Zhang HG, et al., 2020. Fuzzy observer-based repetitive tracking control for nonlinear systems. *IEEE Trans Fuzzy Syst*, 28(10):2401-2415. https://doi.org/10.1109/TFUZZ.2019.2936808

Ye J, Liu LG, Xu JB, et al., 2021. Frequency adaptive proportional-repetitive control for grid-connected inverters. *IEEE Trans Ind Electron*, 68(9):7965-7974. https://doi.org/10.1109/TIE.2020.3016247

Zhang H, Sun Y, 2003. Bode integrals and laws of variety in linear control systems. Proc American Control Conf, p.66-70. https://doi.org/10.1109/ACC.2003.1238915

Zhao T, Tong W, Mao Y, 2023. Hybrid nonsingleton fuzzy strong tracking Kalman filtering for high precision photoelectric tracking system. *IEEE Trans Ind Inform*, 19(3):2395-2408.
https://doi.org/10.1109/TII.2022.3160632

Zheng YS, Cao ZW, Man ZH, et al., 2021. Phase-lead repetitive control of a PMSM with field-oriented feedback linearization and a disturbance observer. Proc 47th Annual Conf of the IEEE Industrial Electronics Society, p.1-4.
https://doi.org/10.1109/IECON48115.2021.9589815

Zhou L, She JH, Zhang XM, et al., 2020. Improving disturbance-rejection performance in a modified repetitive-control system based on equivalent-input-disturbance approach. *Int J Syst Sci*, 51(1):49-60.
https://doi.org/10.1080/00207721.2019.1692954

Zhou X, Mao Y, Zhang H, et al., 2022. Resonance compensation research of tip-tilt mirror's 2-DOF tracking-disturbance rejection problem. *Sens Actuat A Phys*, 346:113837.
https://doi.org/10.1016/j.sna.2022.113837

List of supplementary materials

Proof of Theorem 1
Proof of Theorem 2
Proof of Theorem 3
Proof of Theorem 4
Proof of Theorem 5
Closed-loop experimental result analysis
Experimental results of single-frequency disturbance
Experimental results of multi-frequency disturbance